CASE STUDY

Adaptive Wavelet Simulation of a Flow around an Impulsively Started Cylinder Using Penalisation

Kai Schneider

Laboratoire de Modélisation et Simulation Numérique en Mécanique du CNRS and Centre de Mathématiques et d'lnformatique, Université de Provence, 39 rue Joliot-Curie, 13453 Marseille Cedex 9, France
E-mail: kschneid@cmi.univ-mrs.fr

and

Marie Farge

Laboratoire de Météorologie Dynamique du CNRS, Ecole Normale Supérieure, 24 rue Lhomond, 75231 Paris, Cedex 05, France
E-mail: farge@lrnd.ens.fr

Abstract—We present an adaptive wavelet method to integrate the velocity–vorticity formulation of the two-dimensional Navier–Stokes equations coupled with a penalisation technique to handle efficiently solid boundaries of arbitrary shape. We demonstrate the validity of this method, called coherent vortex simulation (CVS), to compute the flow around an impulsively started cylinder at high Reynolds number and compare the results with a classical vortex method. © 2002 Elsevier Science (USA)

Key Words: adaptive wavelet methods; Navier–Stokes equations; turbulence; bluff body flows; penalisation.

1. INTRODUCTION

The computation of turbulent flows in complex geometries is one of the main challenges in computational fluid dynamics. Hereby the grid generation and adaption play a crucial role. Furthermore turbulent flows are characterized by a wide range of spatial and temporal scales. Hence, multiscale techniques are a suitable tool to get insights into the physics of turbulence. Wavelets have been used so far for analyzing, modeling, and computing turbulent flows; for a review we refer, e.g., to [4–6, 13, 14]. Recently, several adaptive wavelet methods have been developed to solve the two-dimensional Navier–Stokes equations [3, 8, 9, 15, 16]. All presented methods suffer from the drawback that they are limited to simple geometries, i.e., squares or rectangles, mostly assuming periodic boundary conditions.

The penalisation technique, introduced by Arquis and Caltagirone [2], offers an elegant solution to take into account complex geometries. Therewith walls or solid obstacles, even if their shape varies in time, are modelled as a porous medium with porosity η tending to zero. A mathematical justification proving convergence of this physically based approach has been given by Angot *et al.* [1]. This technique has been applied in the context of low order methods (finite difference/volume schemes, e.g., [11]) and also with spectral methods, e.g., [7, 10]. The motivation for coupling the penalisation technique with an adaptive wavelet solver comes from the fact that adaptive wavelet methods automatically refine the grid in regions of strong gradients. Hence, we expect the solver to adapt automatically, not only to the evolution of the flow, but also to the geometry.

After a short presentation of the governing equations together with the penalisation method, we present the adaptive wavelet scheme for the penalized equations. For more details on the numerical scheme we refer to [6, 9, 17]. To validate this new method, called coherent vortex simulation (CVS), we study a prototype of unsteady separated flows, an impulsively started cylinder at high Reynolds number. We illustrate the self-adaptive grid evolution and compare the results with these obtained with a vortex method [12]. Finally, we give some conclusions and perspectives for turbulence modelling.

2. PENALISATION MEETS WAVELETS

In this section we present the governing equations together with the penalisation technique and introduce its coupling with the adaptive wavelet method.

2.1. Physical Problem

The vorticity transport equation

$$\partial_t \omega + \vec{v} \cdot \nabla \omega - \nu \nabla^2 \omega = 0 \tag{1}$$

describes the unsteady incompressible flow of a viscous fluid, where $\vec{v}(\vec{x}, t) = (u(x, y, t), v(x, y, t))$ is the velocity, $\omega = \nabla \times \vec{v}$ is the vorticity, and ν is the kinematic viscosity. The incompressibility, i.e., $\nabla \cdot \vec{v} = 0$, together with the definition of vorticity, implies that $\vec{v}$ is related to ω by the Biot–Savart relation

$$\nabla^2 \vec{v} = \nabla^\perp \omega, \tag{2}$$

with $\nabla^\perp = (-\partial y, \partial x)$. By considering a flow around a solid obstacle Ω_s (here a cylinder) translating with velocity $\vec{V}_0$, the velocity of the fluid is equal to the velocity of the obstacle at its boundary; i.e., $\vec{v}|_{\partial \Omega_s} = \vec{V}_0$. Far from the obstacle, for $|\vec{x}| \to \infty$, we have $\vec{v}(\vec{x}) \to \vec{V}_\infty$, where $\vec{V}_\infty$ is the free-stream velocity.

The Reynolds number of the flow is defined based on the size of the obstacle D (here the diameter of the cylinder) and the mean velocity $\vec{V} = \vec{V}_0 - \vec{V}_\infty$; i.e., $Re = |\vec{V}|D/\nu$. The time is non-dimensionalized with the radius ($R = D/2$) of the cylinder, $T = |\vec{V}|t/R$. Prandtl's classical wall law yields for the boundary layer a thickness $\delta \propto 1/\sqrt{Re}$, which thus requires a strong grid refinement near the wall.

2.2. The Penalisation Technique

The physical idea of the penalisation technique is to model solid walls or obstacles as a porous medium with porosity η tending to zero [2]. The complex geometry is then simply described by a mask function $\chi(\vec{x})$ set to 1 inside the solid regions and to 0 elsewhere. Hence, the penalisation method can also take into account obstacles with time-varying shapes by simply introducing a time-varying mask function. The Navier–Stokes equations are modified by adding a supplementary term containing the mask function. For $\eta \to 0$ the flow evolution is governed by Navier–Stokes equations in the fluid regions and by d'Arcy law (velocity proportional to pressure gradient) in solid regions where the obstacles or walls are.

For an impulsively started obstacle with velocity $\vec{V}_0$ and free-stream velocity $\vec{V}_\infty$ we obtain in vorticity–velocity formulation

$$\partial_t \omega + (\vec{v} + \vec{V}_\infty) \cdot \nabla \omega - \nu \nabla^2 \omega + \nabla \times \left(\frac{1}{\eta} \chi (\vec{v} - \vec{V}_0) \right) = 0 \tag{3}$$

with

$$\chi_{\Omega_s}(\vec{x}) = \begin{cases} 1 & \text{for } \vec{x} \in \vec{\Omega}_s \\ 0 & \text{else.} \end{cases} \tag{4}$$

It has been shown rigorously that the above equations converge in the limit when η tends to zero towards the Navier–Stokes equations with no-slip boundary conditions, with order $\eta^{3/4}$ inside the obstacle and with order $\eta^{1/4}$ elsewhere [1]. In numerical simulations an improved convergence of order η has been reported [1, 10].

To compute the resulting forces $\vec{F}$ on the obstacle, the penalized velocity has to be integrated over the obstacle's volume [1]

$$\vec{F} = \lim_{\eta \to 0} \int_{\Omega_s} \nabla P_\eta \, d\vec{x} = -\lim_{\eta \to 0} \frac{1}{\eta} \int_{\Omega_s} \vec{V}_\eta \, d\vec{x} = \int_{\partial \Omega_s} S(\vec{V}, P) \cdot \vec{n} \, d\gamma, \tag{5}$$

where Ω_s denotes the volume of the obstacle, $\partial \Omega$ denotes its boundary, $\vec{n}$ denotes its outer normal pressure and $S(\vec{V}, P) = (1/2\nu)(\nabla \vec{V} + (\nabla \vec{V})^{\mathrm{T}}) - PI$ is the stress tensor with I the identity. Therefore the drag and the lift (forces parallel and perpendicular to $\vec{V}_0$, respectively) induced by the obstacle are easy to compute as volume integrals instead of contour integrals.

2.3. Adaptive Wavelet Scheme

To solve (3) numerically we first discretize the equations in time using semi-implicit finite differences, i.e., Euler–backwards for the viscous term and Adams–Bashforth extrapolation for the nonlinear term, both of second order.

We obtain

$$(\gamma I - \nu \nabla^2) \omega^{n+1} = \frac{4}{3} \gamma \omega^n - \frac{1}{3} \gamma \omega^{n-1} - \nabla \cdot (\omega^* (\vec{v}^* + \vec{V}_\infty)) + \nabla \times \left(\frac{1}{\eta} \chi (\vec{v}^* - \vec{V}_0) \right), \tag{6}$$

where

$$\omega^* = 2\omega^n - \omega^{n-1} \qquad \text{and} \qquad \vec{v}^* = 2\vec{v}^n - \vec{v}^{n-1}, \tag{7}$$

with time step Δt, $\gamma = 3/(2\Delta t)$.

For spatial discretization we use a Petrov–Galerkin scheme. Therefore the vorticity is developed into a set of trial functions and the minimization of the weighted residual of (6) requires that the projection onto a space of test functions vanishes. As space of trial functions we employ a two-dimensional multiresolution analysis (MRA) and develop ω^n at time step n into an orthonormal wavelet series

$$\omega^n(x,y) = \sum_j \sum_{k_x=0}^{2^j-1} \sum_{k_y=0}^{2^j-1} \sum_{\mu=1,2,3} \langle \omega^n, \psi_{j,k_x,k_y}^\mu \rangle \psi_{j,k_x,k_y}^\mu(x,y). \tag{8}$$

The test functions θ_{j,i_x,i_y}^μ are defined as solutions of the linear part of Eq. (6):

$$(\gamma I - \nu \nabla^2)\theta_{j,i_x,i_y}^\mu = \psi_{j,i_x,i_y}^\mu. \tag{9}$$

This avoids assembling the stiffness matrix and solving a linear equation at each time step. The functions θ, called vaguelettes, are explicitly calculated and have localization properties similar to those of wavelets [9]. The solution of (6) therewith reduces to a simple change of basis

$$\tilde{\omega}_{j,i_x,i_y}^{\mu,n+1} = \langle \omega^{n+1}, \psi_{j,i_x,i_y}^\mu \rangle = \left\langle \left(\frac{4}{3}\gamma\omega^n - \frac{1}{3}\gamma\omega^{n-1} - \nabla \cdot (\omega^*(\vec{v}^* + \vec{V}_\infty)) \right. \right.$$
$$\left. \left. + \nabla \cdot \left(\frac{1}{\eta}\chi(\vec{v}^* - \vec{V}_0) \right) \right), \theta_{j,i_x,i_y}^\mu \right\rangle. \tag{10}$$

An adaptive discretization is obtained by applying at each time step a nonlinear wavelet thresholding technique, retaining only wavelet coefficients $\tilde{\omega}_{j,i_x,i_y}^{\mu,n}$ with absolute value above a given threshold $\epsilon = \epsilon_0\sqrt{Z}$, where ϵ_0 is a constant and $Z = \frac{1}{2}\int |\omega(\vec{x})|^2 d\vec{x}$ the entropy. For the next time step the index coefficient set (which addresses each coefficient in wavelet space) is determined by adding neighbours to the retained wavelet coefficients. Consequently only those coefficients $\tilde{\omega}$ in (10) belonging to this extrapolated index set are computed using the adaptive vaguelette decomposition [9]. The nonlinear term $-\nabla \cdot (\omega^*(\vec{v} + \vec{V}_\infty^*)) + \nabla \times (\frac{1}{\eta}\chi(\vec{v}^* - \vec{V}_0))$ is evaluated by partial collocation on a locally refined grid. The vorticity ω^* is reconstructed in physical space on an adaptive grid from its wavelet coefficients $\tilde{\omega}^*$ using the adaptive wavelet reconstruction algorithm [9]. From the adaptive vaguelette decomposition with $\theta = (\nabla^2)^{-1}\psi$, we solve $\nabla^2\Psi^* = \omega^*$ to get the stream function $\tilde{\Psi}^*$ and reconstruct Ψ^* on a locally refined grid. By means of centered finite differences of fourth order we compute $\nabla\omega^*$, $\vec{v}^* = (-\partial_y\Psi^*, \partial_x\Psi^*)$ and $\nabla \times (\frac{1}{\eta}\chi(\vec{v}^* - \vec{V}_0))$ on the adaptive grid. Subsequently, the nonlinear term is summed up pointwise and finally (10) is solved using the adaptive vaguelette decomposition.

3. NUMERICAL RESULTS

Here we present an application of the CVS method to compute a flow past an impulsively started cylinder at $Re = 3000$, as proposed in [12]. The numerical difficulty comes from the fact that, due to the impulsive start, a thin boundary layer develops and thus the drag coefficient exhibits a $t^{-1/2}$ singularity. The freestream velocity V_∞ is set to zero and the obstacle's velocity $\vec{V}_0$ is set to $(1,0)$ at $t = 0^+$. The computational domain is $[0, 4D]^2$, where $D = 1$ is the diameter of the cylinder which is centered in the domain. We use
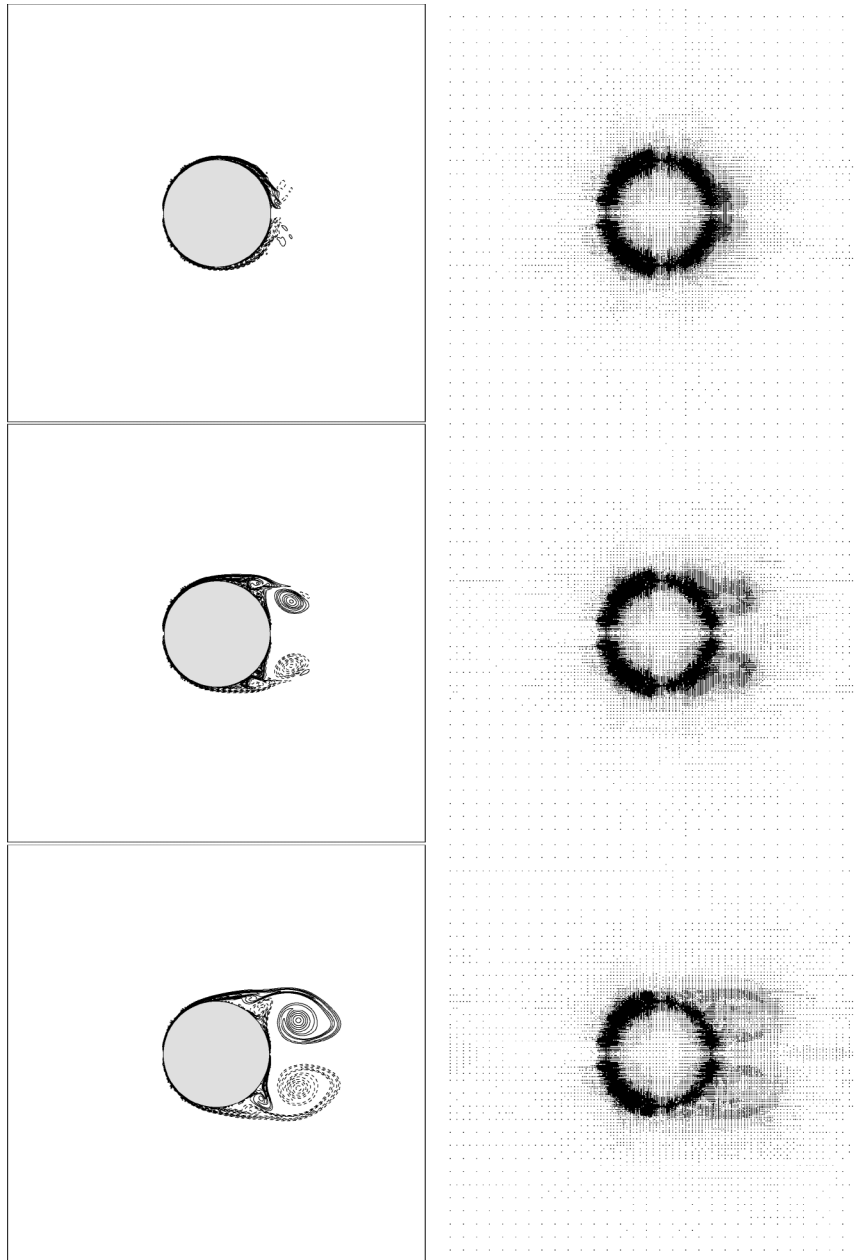
FIG. 1. CVS of an impulsively started cylinder at $Re = 3000$. Left: Isolines of vorticity at $T = 1, 3, 5$. Right: Center of the active wavelet coefficients in physical space. Note that at $T = 1, 3, 5$ only 18,781, 20,089, 20,764 out of $512^2 = 262{,}144$ wavelet modes are used.

a resolution of 512^2, with a time step $\Delta t = 5 \cdot 10^{-4}$, a threshold parameter $\epsilon_0 = 10^{-5}$, and a penalisation parameter $\eta = 10^{-3}$. In Fig. 1 we show isolines of the vorticity field for three instants (left) together with the corresponding locally refined grid (right). We observe that the grid automatically adapts to the obstacle and follows the flow evolution, since it is refined in regions of strong vorticity gradients. A comparison of the time evolution of
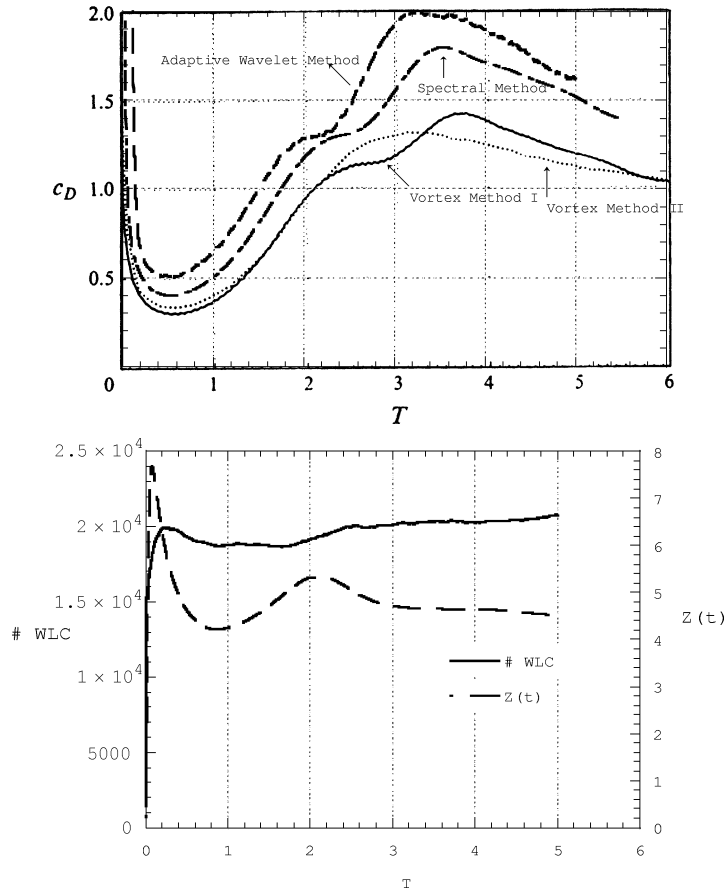
FIG. 2. Top: Comparison of the time evolution of the drag coefficient between the adaptive wavelet method (CVS), a spectral method with penalisation (DNS), and two different vortex methods [12]. Bottom: Time evolution of the number of active wavelet modes (solid line) and of the total enstrophy Δ^2-norm of norticity (dashed line).

the drag coefficient, computed using the CVS method, direct numerical simulation (DNS) with penalisation [17], and two different vortex methods [12], top shows the validity of the adaptive wavelet method (Fig. 2, top). Note that compared with a spectral method (DNS) only about 8% of the total number of modes are used (Fig. 2, bottom).

4. CONCLUSION

We have presented an adaptive wavelet method called CVS to compute two-dimensional turbulent flows in complex geometries using a penalisation technique. Computing a flow behind an impulsively started cylinder at Reynold number 3000, we have shown the validity of the wavelet method. We illustrated the feature of automatic grid adaption and found a good prediction of the drag coefficient compared with two classical vortex methods. In future work we will increase the threshold and develop a turbulence model to simulate the effect of the discarded wavelet modes onto the retained modes, as done in [6] for a mixing layer.

REFERENCES

1. P. Angot, C. H. Bruneau, and P. Fabrie, A penalisation method to take into account obstacles in viscous flows, *Numer. Math.* **81** (1999), 497–520.

2. E. Arquis and J. P. Caltagirone, Sur les conditions hydrodynamique au voisinage d'une interface millieux fluide–millieu poreux: application à la convection naturelle, *C.R. Acad. Sci. Paris II* **299** (1984), 1–4.

3. Ph. Charton and V. Perrier, A pseudo-wavelet scheme for the two-dimensional Navier–Stokes equations, *Mat. Apli. Comput.* **15** (1996), 139–160.

4. M. Farge, Wavelet transforms and their applications to turbulence, *Annual Rev. Fluid Mech.* **24** (1992), 395–457.

5. M. Farge, K. Schneider, and N. Kevlahan, Non-Gaussianity and coherent vortex simulation for two-dimensional turbulence using an adaptive orthonormal wavelet basis, *Phys. Fluids* **11**, No. 8 (1999), 2187–2201.

6. M. Farge and K. Schneider, Coherent vortex simulation (CVS), a semi-deterministic turbulence model using wavelets, *Flow, Turbulence Combust.* **66**, No. 4 (2001), 393–426.

7. M. Forrestier, R. Pasquetti, and R. Peyret, Calculations of 3D wakes in stratified fluids, presented at ECCOMAS 2000.

8. J. Fröhlich and K. Schneider, Numerical simulation of decaying turbulence in an adaptive wavelet basis, *Appl. Comput. Harmon. Anal.* **3** (1996), 393–397.

9. J. Fröhlich and K. Schneider, An adaptive wavelet–vaguelette algorithm for the solution of PDEs, *J. Comput. Phys.* **130** (1997), 174–190.

10. N. Kevlahan and J.-M. Ghidaglia, Computation of turbulent flow past an array of cylinders using a spectral method with Brinkman penalization, *European J. Mech. B Fluids* **20** (2001), 333–350.

11. K. Khadra, S. Parneix, P. Angot, and J.-P. Caltagirone, Fictious domain approach for numerical modelling of Navier–Stokes equations, *Internat. J. Numer. Methods Fluids* **34** (2000), 651–684.

12. P. Koumoutsakos and A. Leonard, High resolution simulations of the flow around an impulsively started cylinder using vortex methods, *J. Fluid Mech.* **296** (1995), 1–38.

13. C. Meneveau, Analysis of turbulence in the orthonormal wavelet representation, *J. Fluid Mech.* **232** (1991), 469.

14. K. Schneider and M. Farge, Computing and analysing turbulent flows using wavelets, *in* "Wavelet Transforms and Time-Frequency Signal Analysis" (L. Debnath, Ed.), pp. 181–216, Birkhäuser, Boston, 2001.

15. K. Schneider and M. Farge, Numerical simulation of a mixing layer in an adaptive wavelet basis, *C.R. Acad. Sci. Paris Sér. II* **328** (2000), 263–269.

16. K. Schneider, M. Farge, F. Koster, and M. Griebel, "Adaptive Wavelet Methods for the Navier–Stokes Equations," Notes on Numerical Fluid Mechanics (E. H. Hirschel, Ed.), pp. 303–318, Springer-Verlag, Berlin/New York, 2001.

17. K. Schneider, An adaptive wavelet method for 2D turbulence in complex geometries, preprint, CMI Université de Provence, Marseille, 2002.